Available online at www.sciencedirect.com
ScienceDirect
Renewable Energy 32 (2007) 118–140
RENEWABLE ENERGY
www.elsevier.com/locate/renene

Data Bank

The impact of array inclination and orientation on the performance of a grid-connected photovoltaic system

Jayanta Deb Mondol[a,*], Yigzaw G. Yohanis[a], Brian Norton[b]

[a]*School of the Built Environment, University of Ulster, Newtownabbey, Northern Ireland, BT37 0QB, UK*
[b]*Dublin Institute of Technology, Aungier Street, Dublin 2, Ireland*

Received 8 March 2006; accepted 24 May 2006
Available online 18 July 2006

Abstract

The impact of PV surface orientation and inclination on grid-connected photovoltaic system performance under maritime climates was investigated using validated TRNSYS simulations. Insolation, PV output, PV efficiency, inverter efficiency, system efficiency, performance ratio (PR) and PV savings were estimated annually, seasonally and on monthly bases for various surface inclinations and orientations. Incident insolation and PV output were maximum for a surface with inclination 30° facing due south and minimum for a vertical surface with orientation 90° east or west from south. The monthly optimum collection angle maximising incident insolation varied from 10° to 70°. For the particular location and system studied, the maximum annual PV efficiency, the inverter efficiency, the PR and the system efficiency were for a south-facing surface with an inclination of 20°. For a horizontal surface, the monthly variation of system parameters was significant over a year. For time-dependent tariff rates, the annual PV savings were higher for a system oriented with same orientation towards the west than east from south while for constants tariff rates, the PV savings was the same for east or west orientation from south.
© 2006 Elsevier Ltd. All rights reserved.

Keywords: Grid-connected photovoltaic; Orientation; Inclination; Insolation; PV output; Performance ratio

*Corresponding author. Tel.: +44 2890 368037; fax: +44 2890 368239.
E-mail address: jd.mondol@ulster.ac.uk (J.D. Mondol).

0960-1481/$ - see front matter © 2006 Elsevier Ltd. All rights reserved.
doi:10.1016/j.renene.2006.05.006

Nomenclatures

A	PV array area (m^2)
$E_{AC\ \gamma,\beta}$	annual total inverter output for any surface (MJ)
$E_{DC\ \gamma,\beta}$	annual total PV output for any surface (MJ)
$E_{DC,\gamma_{max},\beta_{max}}$	maximum annual total PV output(MJ)
$E_{N,PV}$	annual total PV output for any surface normalised with respect to maximum annual total PV output
$E_{N,PV,S}$	seasonal PV output normalised with respect to PV rated capacity ($MJ\,kW_p^{-1}$)
$E_{S,DC,\gamma,\beta}$	seasonal PV output for any surface (MJ)
$I_{\gamma,\beta}$	annual total in-plane insolation for any surface ($MJ\,m^{-2}$)
$I_{\gamma_{max},\beta_{max}}$	maximum annual total in-plane insolation ($MJ\,m^{-2}$)
k_0, k_1, k_2	correlation coefficients
P_{inv}	AC output power from an inverter (W)
$P_{inv,n}$	normalised inverter output power
$P_{inv,rated}$	inverter's rated input capacity (kVA)
P_{pv}	DC input power to an inverter (W)
$P_{PV,rated}$	rated capacity of PV array (kW_p)
$P_{pv,n}$	normalised inverter input power
PR	performance ratio (%)
Y_f	annual final yield ($h\,year^{-1}$)
Y_r	annual reference yield ($h\,year^{-1}$)
β	surface tilt angle (deg.)
γ	surface azimuth angle (deg.)
ε_I	variation of annual total in-plane insolation for any surface orientation and inclination from the annual total maximum insolation (%)
ε_{PV}	variation of annual total PV output for any surface orientation and inclination from the annual total maximum PV output (%)
$\eta_{inv,\gamma,\beta}$	inverter efficiency for any surface (%)
$\eta_{PV,\gamma,\beta}$	PV efficiency for any surface (%)
$\eta_{s,\gamma,\beta}$	system efficiency for any surface (%)

1. Introduction

A photovoltaic (PV) system should be installed to maximise the solar contribution to a particular load. Optimum PV inclination and orientation depends on local climate, load consumption temporal profile and latitude [1–3]. Generally, a surface with tilt angle equal to the latitude of a location receives maximum insolation. However, some locations experience a weather pattern where winter is typically cloudier than summer or the average morning and afternoon insolation is not symmetric. The maximum available energy may then be received by a surface whose azimuth angle is either east or west of due south (in the Northern hemisphere). The optimum tilt angle is thus site dependent and calculation of this angle requires solar radiation data for that particular site for the whole year. Normally, during summer, the incident insolation is maximised for a surface with

an inclination 10–15° less than the latitude and, during winter, 10–15° more than the latitude [4].

For commercial buildings, the electricity tariff depends on the time of use, based on "off-peak" and "on-peak" time periods. PV displaces more expensive utility electricity and is more viable economically when the PV system reduces the peak load demand. For residential users who pay a constant utility rate, the best PV surface inclination and orientation leads to the maximum total annual PV generation.

Various studies have been carried out to investigate the effect of orientation and inclination on the PV system performance [5–13]. Helmke et al. [5] observed that PV peak power was higher in winter than summer for a vertical south-facing surface due to lower sun angle in Northern hemisphere. Nakamura et al. [6] reported that PV efficiency decreased by 1% for a horizontal surface than for a 30°-tilted surface due to variation of solar incident angle, solar spectrum and dirt on the module surface for a location at latitude 34.45°N and longitude 137.4°. An experimental study showed that for a location with latitude 35.7°N and longitude 51.4°, the maximum PV energy was produced by a surface with tilt angle of 29° [7]. Oladiran [8] found that the mean annual insolation decreased with azimuth angle for a surface with inclination of 10° above the latitude angle but increased for a surface with inclination 10° less than the latitude angle. Akhmad et al. [9] observed that the voltage at the maximum power point reduced to half when the azimuth angle was between 0° and 15° whereas, output power declined by 75% when PV array was oriented 90° east and west from due south. Hiraoka et al. [10] reported that for a location with latitude 34.5°N and longitude 135.5°, a north-oriented polycrystalline Si PV array generated 67% more electricity compared to a south-oriented crystalline Si PV array during summer. Balouktsis et al. [11] estimated that the annual PV output was 94–96% of the maximum annual PV output if the optimum tilt angle was adjusted once a year and 99% of the maximum annual PV output if the optimum angle is adjusted twice a year. Kacira et al. [12] found that for a location with latitude 37°N and longitude 38°, the optimum tilt angle varied 13–61° from summer to winter. Hussein et al. [13] reported that the maximum annual PV efficiency was 10.8% for an east-facing vertical surface and the minimum was 9.1% for a south-facing 30°-tilted surface, and the annual PV yields were 95% and 41% of the optimum annual PV yield for horizontal and vertical surfaces, respectively.

This work investigates the impact of PV orientation and inclination on annual, seasonal and monthly bases on the following variables: incident insolation, PV output, PV efficiency, system efficiency, inverter efficiency, performance ratio (PR) and PV savings. The seasons are defined as winter (December, January and February); spring (March, April and May); summer (June, July and August) and autumn (September, October and November).

2. Description of the PV system

The study was conducted on a grid-connected PV system located in Northern Ireland under maritime climates. The PV array is installed on the roof of the ECOS Millennium Environmental Centre (latitude: 54°52′N and longitude: 6°17′W) inclined at 45°-facing due south. The 13 kW_p rated PV array consists of 119 single-crystalline PV modules. The DC electricity produced by the PV array is converted to AC electricity by a 13-kVA-rated inverter, connected to 415-V AC, 3-phase building's electrical network. It has been shown

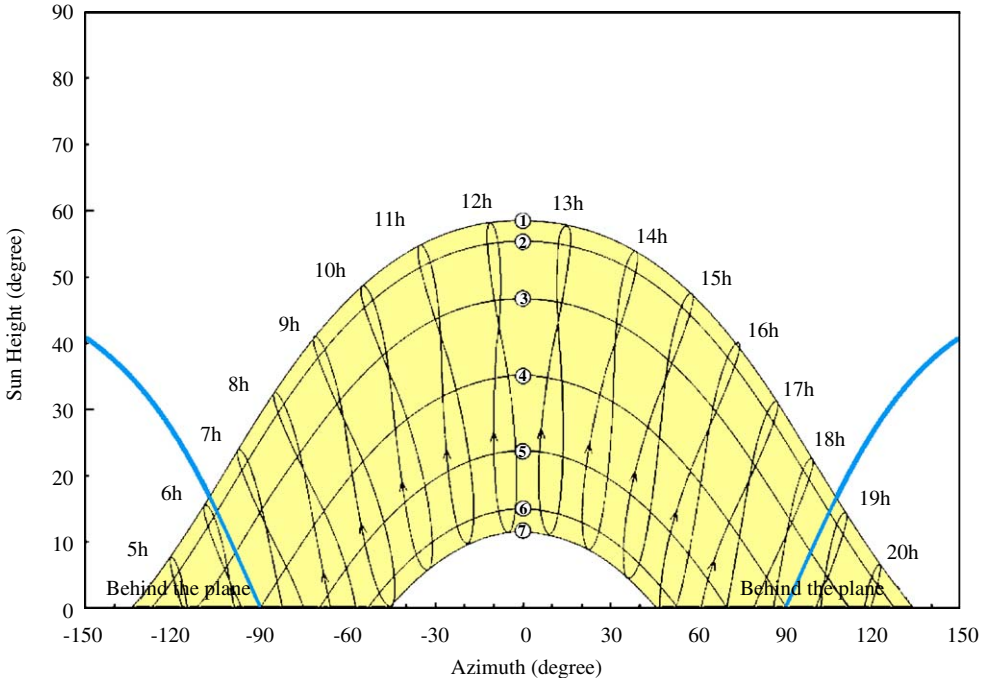

Fig. 1. Sun-path diagram at the ECOS Centre (1) 22 June, (2) 22 May–23 July, (3) 20 April–23 August, (4) 20 March–23 September, (5) 21 February–23 October, (6) 19 January–22 November and (7) 22 December.

previously that the performance of this PV system is representative of typical installations [14]. Fig. 1 illustrates the sun path diagram for the location of the ECOS Centre. The solar altitude angle at the solar noon varies from 12° to 60° from winter to summer.

3. TRNSYS simulation

The variables were evaluated using TRNSYS [15]. The tilt angle (β) was varied from 0° to 90° and surface azimuth angle (γ) from 90° east and west from south at 10° increments, respectively. In addition, the tilt angle 45° was also considered for this exercise to represent the actual inclination of the PV array installed at the ECOS Centre. Therefore, a matrix of 209 TRNSYS simulations was constructed to calculate the variables. The TRNSYS [15] components used were 'data reader' (Type 9), 'radiation processor' (Type 16), 'PV array' (Type 94), 'holiday calculator' (Type 95), 'utility rate schedule processor' (Type 96), 'quantity integrator' (Type 24) and an inverter component (Type 146) developed for this study.

The 'data reader' [15] read data from a data file which contains hourly horizontal global and diffuse insolation and ambient temperature data obtained from the meteorological station located at Aldergrove, Northern Ireland, latitude 54°. The 'radiation processor' component [15] was used to calculate in-plane insolation from horizontal global and diffuse insolation using Liu and Jordan's [16] isotropic sky-tilted surface radiation model. Ground reflection was assumed to be constant and equal to 0.2. To simulate

single-crystalline PV module, the 'four-parameter' equivalent circuit was used in the 'PV array' component [15]. The four parameters were (i) module photocurrent at reference conditions, (ii) diode reverse saturation current at reference conditions, (iii) an empirical PV curve-fitting factor, and (iv) module series resistance. The 'incidence angle of modifier' was employed to calculate reflection losses due to incidence angle of irradiance on the array surface. PV module and array characteristic parameters used in this component are shown in Table 1.

A new component (Type 146) has been developed to predict inverter output using the following correlation [17]:

$$P_{\mathrm{inv,n}} = k_0 + k_1 P_{\mathrm{pv,n}} + k_2 P_{\mathrm{pv,n}}^2, \tag{1}$$

where

$$P_{\mathrm{pv,\,n}} = \frac{P_{\mathrm{pv}}}{P_{\mathrm{inv,\,rated}}}, \quad \text{and} \quad P_{\mathrm{inv,\,n}} = \frac{P_{\mathrm{inv}}}{P_{\mathrm{inv,\,rated}}} \tag{2}$$

where $P_{\mathrm{pv,n}}$ and $P_{\mathrm{inv,n}}$ are the normalised inverter input and output power, respectively. P_{pv} and P_{inv} are PV and inverter output power. $P_{\mathrm{inv,rated}}$ is the rated inverter input capacity. k_0, k_1 and k_2 are correlation coefficients.

The 'holiday calculator' component [15] identified the day, month, week and hour to enable calculation of the utility savings at any particular time interval. The PV savings was calculated from hourly electricity tariff rate and hourly used PV energy using TRNSYS 'utility rate schedule processor' component [15], which reads utility rate at any time step from a utility rate schedule data file. A new TRNSYS component was developed to generate a data file based on time dependence as well as flat tariff rates and was included in the TRNSYS main programme. Table 2 shows the two types of utility rate schedules used [18]. Output of the inverter is considered as the PV energy utilised by the building.

Table 1
Characteristic parameters of the PV module and array used in the PV simulation

Parameter	Value
Module short circuit current at reference conditions	3.45 (A)
Module open circuit voltage at reference conditions	43.5 (V)
Temperature at reference conditions	298 (K)
Irradiance at reference conditions	1000 ($\mathrm{W\,m^{-2}}$)
Maximum power point voltage at reference conditions	35.0 (V)
Maximum power point current at reference conditions	3.15 (A)
Temperature coefficient of short circuit current	4.0×10^{-4} ($\mathrm{A\,K^{-1}}$)
Temperature coefficient of open circuit voltage	-3.4×10^{-3} ($\mathrm{V\,K^{-1}}$)
Module temperature at NOCT conditions	313 (K)
Ambient temperature at NOCT conditions	293 (K)
Insolation at NOCT conditions	800 ($\mathrm{W\,m^{-2}}$)
Transmittance–absorptance product at normal incidence	−0.91
Semiconductor bandgap	1.12 (eV)
Number of cells in the module connected in series	72
Number of modules in each sub-array in series	17
Number of sub arrays in parallel	7
Individual module area	0.87 ($\mathrm{m^2}$)

Table 2
Utility rate schedules

Type of Tariff	Time period	Rate (p kWh^{-1})
Type 1	8 am to 8.30 pm (March–October)	6.4
	8 am to 8.30 pm (November, December, January and February)	9.6
	4 pm to 7 pm (November, December, January and February)	48.0
	Evening and night and week end	3.5
Type 2	Flat tariff	9.64

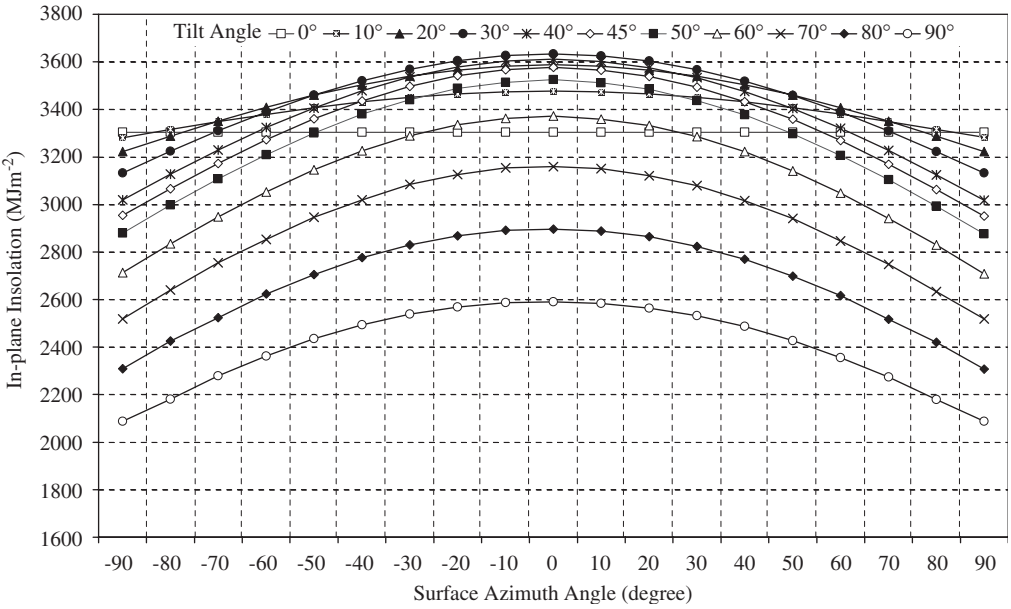

Fig. 2. Variation of annual total insolation as functions of surface azimuth and tilt angles.

Predicted PV and inverter outputs were compared with measured long-term-monitored data at the PV system at the ECOS Centre [17]. It has been found that the predicted PV output agreed closely with measured data and R^2 value that indicates the discrepancy between the measured and predicted results was found to be 0.97. The annual average monthly error between measured and predicted inverter output was 5% [17].

4. Effect of surface inclination and orientation on incident insolation

4.1. Annual insolation

The annual total insolation as functions of surface azimuth and tilt angles depicted in Fig. 2 shows that the maximum annual total insolation is for a south-facing surface with a tilt angle of 30°. The annual total insolation for the surface oriented in the same direction

towards east and west from south is approximately the same, indicating a symmetric distribution of irradiance before and after midday.

The variation of annual total in-plane insolation (ε_I) for different orientations and inclinations from the estimated maximum annual total insolation is calculated as follows:

$$\varepsilon_I = \left(\frac{I_{\gamma_{max},\beta_{max}} - I_{\gamma,\beta}}{I_{\gamma_{max},\beta_{max}}} \right) \times 100\%, \quad (3)$$

where $I_{\gamma_{max},\beta_{max}}$ represents the maximum annual total in-plane insolation and $I_{\gamma,\beta}$ is the annual total in-plane insolation for any surface. Table 3 summarises the variation of annual total insolation (ε_I) calculated using Eq. (3) for different surface inclinations and orientations. For horizontal and vertical south-facing surfaces, the annual total insolations are 9.05% and 28.70%, lower, respectively, than the maximum insolation annually obtained for a 30°-tilted surface facing due south, respectively. The annual total incident insolation is approximately less by 2% than the maximum annual total insolation for surface orientation of 30° east or west from due south indicating that the incident insolation is less affected by surface orientation. For a vertical surface with orientation of 90° east and west from due south, the incident insolation is 42.5% lower than the maximum annual total insolation, whereas for a 10°-tilted surface with the same surface orientation, the annual total insolation is reduced by 9.6%. Fig. 3 illustrates the variation of annual total insolation normalised with respect to the maximum annual total insolation

Table 3
Variation of annual total incident insolation for any surface compared to maximum annual total incident insolation

Azimuth angle (deg.)	Surface tilt angle										
	ε_I (%)										
	0°	10°	20°	30°	40°	45°	50°	60°	70°	80°	90°
−90	9.05	9.69	11.32	13.75	16.88	18.69	20.73	25.31	30.66	36.46	42.55
−80	9.05	8.74	9.52	11.25	13.92	15.60	17.49	21.96	27.32	33.25	39.95
−70	9.05	7.82	7.79	8.89	11.11	12.67	14.44	18.86	24.17	30.52	37.26
−60	9.05	6.97	6.19	6.70	8.52	9.93	11.67	15.97	21.46	27.77	34.97
−50	9.05	6.20	4.76	4.75	6.25	7.50	9.14	13.40	18.88	25.54	32.98
−40	9.05	5.54	3.54	3.10	4.25	5.44	6.96	11.21	16.86	23.60	31.34
−30	9.05	5.01	2.55	1.76	2.65	3.75	5.29	9.46	15.12	22.12	30.10
−20	9.05	4.62	1.84	0.77	1.52	2.52	3.96	8.17	13.95	21.03	29.31
−10	9.05	4.39	1.39	0.18	0.79	1.80	3.28	7.44	13.19	20.44	28.81
0	9.05	4.31	1.24	0.00	0.60	1.55	2.98	7.17	13.04	20.27	28.70
10	9.05	4.39	1.40	0.20	0.84	1.86	3.35	7.53	13.27	20.52	28.90
20	9.05	4.62	1.85	0.82	1.59	2.60	4.05	8.28	14.08	21.17	29.44
30	9.05	5.00	2.56	1.80	2.72	3.84	5.39	9.58	15.25	22.28	30.30
40	9.05	5.53	3.54	3.14	4.32	5.52	7.05	11.32	17.00	23.77	31.54
50	9.05	6.19	4.76	4.79	6.31	7.56	9.22	13.52	19.05	25.75	33.19
60	9.05	6.96	6.19	6.74	8.59	10.01	11.77	16.12	21.66	27.98	35.17
70	9.05	7.81	7.79	8.93	11.18	12.75	14.55	19.04	24.37	30.72	37.41
80	9.05	8.72	9.52	11.29	13.99	15.70	17.62	22.13	27.49	33.37	40.00
90	9.05	9.66	11.32	13.79	16.95	18.78	20.84	25.44	30.66	36.48	42.53

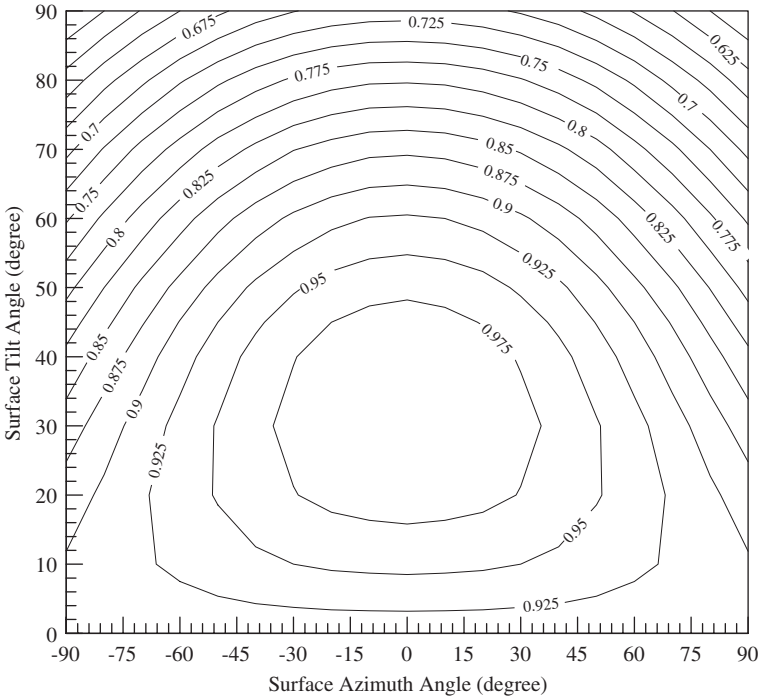

Fig. 3. Distribution of annual total insolation normalised with respect to the annual total maximum insolation value as functions of surface azimuth and tilt angles.

as functions of surface azimuth and tilt angles. The maximum annual total insolation is achieved for a surface with tilt angle less than the local latitude signifying that for this particular location the available insolation in summer is much higher than in winter.

4.2. Seasonal insolation

Fig. 4 illustrates the seasonal distribution of insolation for various surface inclinations and orientations. In winter, the maximum insolation is obtained for a south-facing surface tilted at 60°; for horizontal and vertical surfaces, the incident insolation in winter is approximately 42% and 12%, lower, respectively, than the maximum incident insolation. If the PV surface were oriented to collect maximum insolation in winter, the annual total insolation would be reduced by 12% from the maximum total annual insolation. In summer, the maximum insolation is for a 20°-tilted surface facing due south, approximately 2% and 40% higher than insolation for horizontal and vertical surfaces, respectively. The incident insolation is reduced by approximately 5% for 90° east or west orientation from due south compared with a south-facing surface. In spring and autumn, the maximum insolation is obtained for surfaces inclined at 30° and 50°, respectively. For south-facing vertical and horizontal surfaces, the incident insolation is 20% and 23%, lower, respectively in autumn and 31% and 7% lower in spring than the corresponding seasonal maximum insolation.

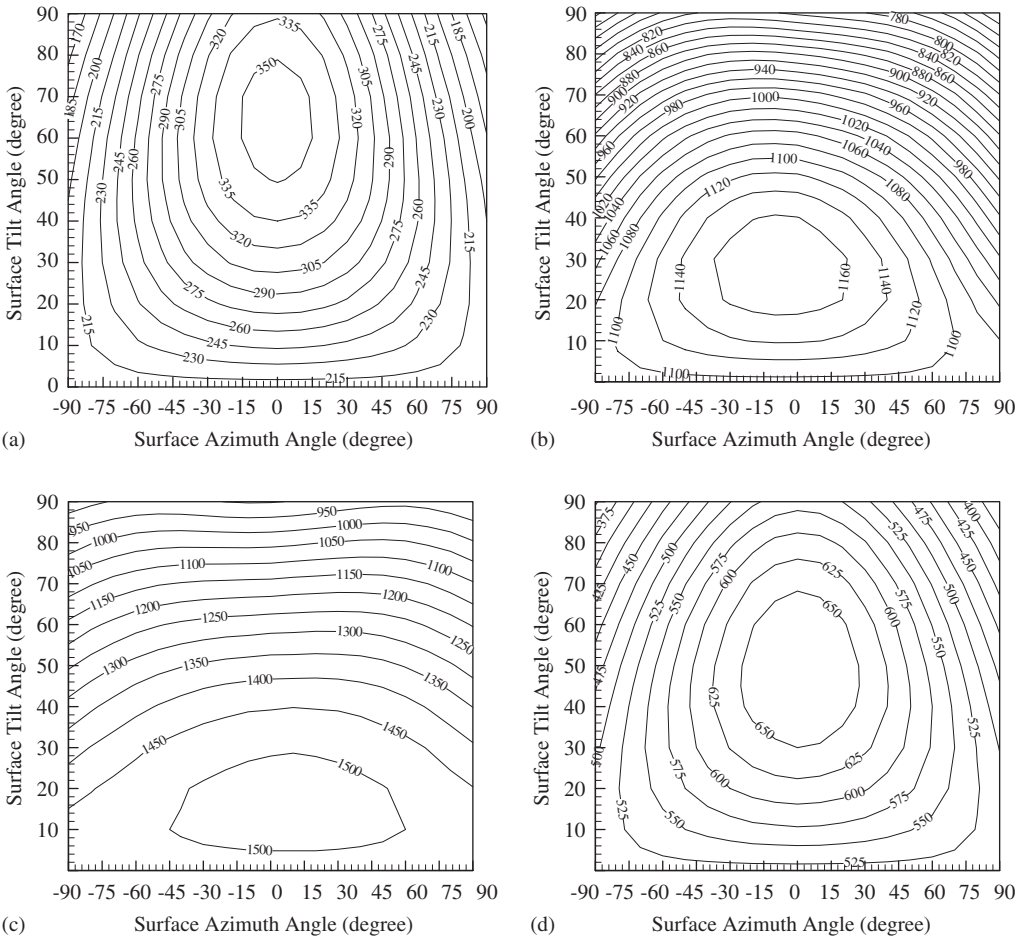

Fig. 4. Seasonal variation of insolation (MJm^{-2}) as functions of surface azimuth and tilt angles: (a) winter, (b) spring, (c) summer and (d) autumn.

4.3. Monthly insolation

Fig. 5 shows the monthly average daily total incident insolation for a south-facing surface with respect to different surface tilt angles. The results show that during winter the amount of insolation on the surface increases for larger tilt angles. In December, January and February, the maximum incident insolation is approximately 4%, 5.5%, 11% higher, respectively, than for a vertical surface and 55%, 47% and 31% higher than for a horizontal surface. In winter, the maximum insolation is achieved for a surface with a tilt angle 15° higher than the local latitude; this corresponds well with previous recommendations [4]. The insolation on vertical and horizontal surfaces are 6% and 45% lower, respectively, than the maximum insolation obtained for a surface with tilt angle of 70° in November. The maximum incident insolation in summer is achieved for a surface with tilt angle approximately 40° lower than the local latitude. In June, July and August, the maximum insolation is achieved for surfaces with tilt angles of 10°, 15° and 20°,

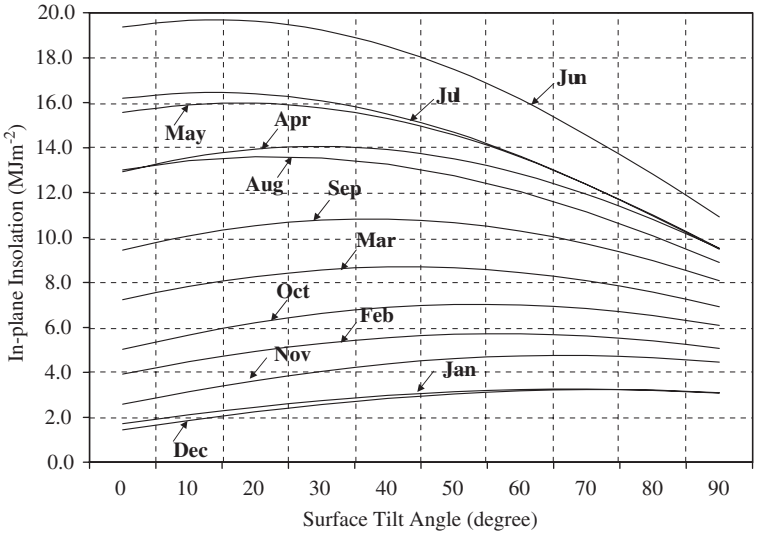

Fig. 5. Monthly average daily total incident insolation as a function of surface tilt angle.

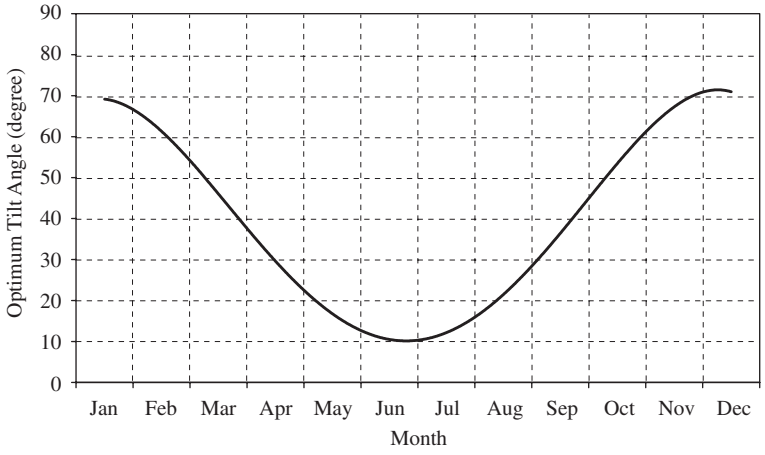

Fig. 6. Monthly optimum PV array surface tilt angle maximising incident insolation.

respectively. The insolation on a vertical surface is approximately 42% lower than the maximum insolation during summer. It has been found that diffuse insolation on a horizontal surface is significant at the ECOS Centre [19]. The diffuse component on an inclined surface decreases with increasing surface tilt. The maximum insolation in September and October are for surfaces with tilt angles of 35° and 50°, respectively. In September and October, the incident insolations on a horizontal surface is 12.7% and 28% and for a vertical surface 25% and 13% lower, respectively, than the respective monthly maximum insolation. The surface tilt angles maximising monthly insolation for a south-facing surface depicted in Fig. 6 shows that the monthly optimum collection angle for incident insolation varies from 10° to 70°.

5. Effect of surface inclination and orientation on PV output

5.1. Annual PV output

The normalised PV output, $E_{N,PV}$ for any surface is as follows:

$$E_{N,\,PV} = \frac{E_{DC,\gamma,\beta}}{E_{DC,\gamma_{max},\beta_{max}}}, \tag{4}$$

where $E_{DC,\gamma,\beta}$ represents annual total PV output for any surface and $E_{DC,\gamma_{max},\beta_{max}}$ is the maximum annual total PV output.

The variation of annual total PV output normalised with respect to the annual total maximum ($E_{N,PV}$) as functions of surface tilt and azimuth angles is shown in Fig. 7. The maximum annual PV output is obtained for a surface with tilt angle of 30° facing due south, i.e., for this surface $E_{N,PV}$ is equal to 1. For vertical and horizontal south-facing surfaces, the normalised factors are 0.6 and 0.9, respectively.

The percentage variation between the maximum annual total PV output and annual total PV output for any surface orientation and inclination (ε_{PV}) is calculated as shown below:

$$\varepsilon_{PV} = \left(\frac{E_{DC,\gamma_{max},\beta_{max}} - E_{DC,\gamma,\beta}}{E_{DC,\gamma_{max},\beta_{max}}}\right) \times 100\%. \tag{5}$$

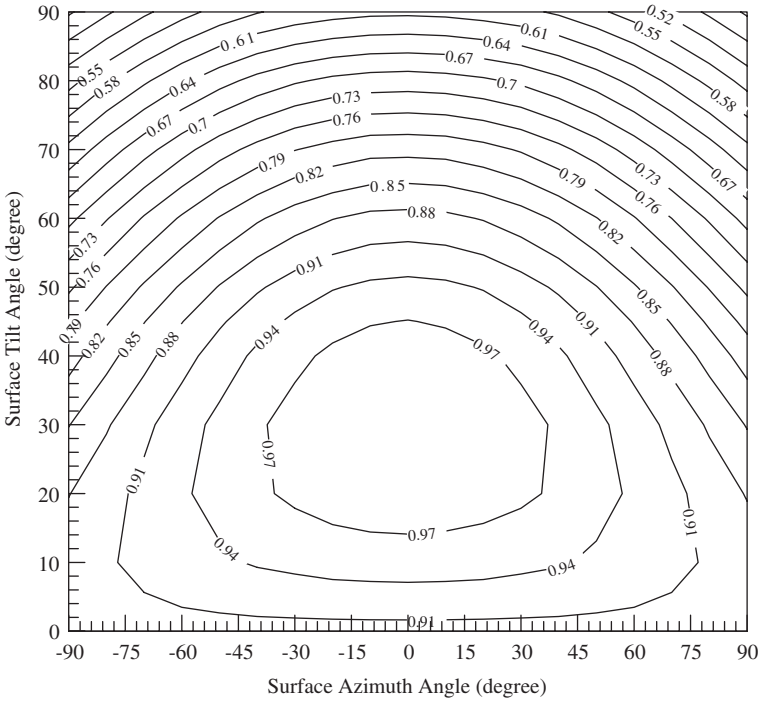

Fig. 7. Distribution of annual total PV output for any surface normalised with respect to the annual total maximum PV output.

Table 4
Percentage variation of annual total PV output normalised with respect to maximum annual total PV output for various surface orientations and inclinations

Azimuth angle (deg.)	Surface tilt angle										
	ε_{PV} (%)										
	0°	10°	20°	30°	40°	45°	50°	60°	70°	80°	90°
−90	9.94	10.39	12.13	15.10	19.23	21.72	24.51	30.84	38.16	46.09	54.44
−80	9.94	9.32	10.12	12.35	15.98	18.30	20.94	27.16	34.50	42.63	51.50
−70	9.94	8.29	8.21	9.75	12.90	15.08	17.59	23.73	31.06	39.52	48.60
−60	9.94	7.34	6.43	7.35	10.07	12.10	14.55	20.57	28.01	36.56	46.07
−50	9.94	6.48	4.86	5.21	7.58	9.45	11.80	17.76	25.24	34.09	43.93
−40	9.94	5.75	3.51	3.40	5.41	7.20	9.44	15.38	22.99	32.00	42.21
−30	9.94	5.16	2.43	1.93	3.67	5.37	7.60	13.45	21.14	30.42	40.97
−20	9.94	4.72	1.64	0.85	2.41	4.02	6.17	12.06	19.86	29.30	40.18
−20	9.94	4.46	1.15	0.20	1.63	3.22	5.38	11.23	19.05	28.68	39.74
0	9.94	4.37	0.99	0.00	1.39	2.94	5.07	10.95	18.86	28.50	39.64
10	9.94	4.46	1.16	0.21	1.66	3.27	5.43	11.29	19.12	28.75	39.82
20	9.94	4.72	1.65	0.89	2.46	4.08	6.24	12.16	19.98	29.46	40.36
30	9.94	5.16	2.45	1.97	3.73	5.45	7.70	13.58	21.31	30.65	41.24
40	9.94	5.75	3.53	3.44	5.49	7.29	9.55	15.53	23.20	32.28	42.53
50	9.94	6.48	4.88	5.27	7.66	9.55	11.93	17.95	25.51	34.41	44.26
60	9.94	7.34	6.46	7.41	10.18	12.23	14.71	20.81	28.31	36.87	46.37
70	9.94	8.29	8.24	9.82	13.02	15.23	17.78	23.99	31.35	39.80	48.81
80	9.94	9.32	10.16	12.43	16.11	18.47	21.15	27.40	34.73	42.81	51.62
90	9.94	10.38	12.17	15.19	19.37	21.88	24.68	31.03	38.23	46.17	54.47

The values of ε_{PV} for various surface inclinations and orientations are shown in Table 4. The results show that ε_{PV} for horizontal and vertical south-facing surfaces are 9.94% and 39.64%, respectively. The lowest PV output, approximately 54.4% lower than the maximum, is found for a vertical surface with orientation 90° east or west from due south. For a 45°-tilted surface, the actual PV inclination of the ECOS PV system, the annual total PV output is 2.9% lower than the maximum value. Table 4 shows that the annual total PV generation is symmetrical towards east and west from south.

5.2. Seasonal PV output

Fig. 8 illustrates the seasonal PV output (in MJ) normalised with respect to PV-rated capacity (in kW_p) for various surface orientations and inclinations. The normalised seasonal PV output, $E_{N,PV,S}$ for any surface is given by

$$E_{N,\,PV,\,S} = \frac{E_{S,\,DC,\,\gamma,\beta}}{P_{PV,\,rated}}, \tag{6}$$

where $E_{S,DC,\gamma,\beta}$ is seasonal PV output for any surface. $P_{PV,rated}$ is the PV-rated capacity which is 13 kW_p for the present system. The results show that in winter, the maximum annual PV output is for the 60°-tilted surface facing south and for horizontal and vertical surfaces, PV output decline approximately by 49% and 10%, respectively, from the maximum over this period. In winter, the solar elevation at noon and the sunshine

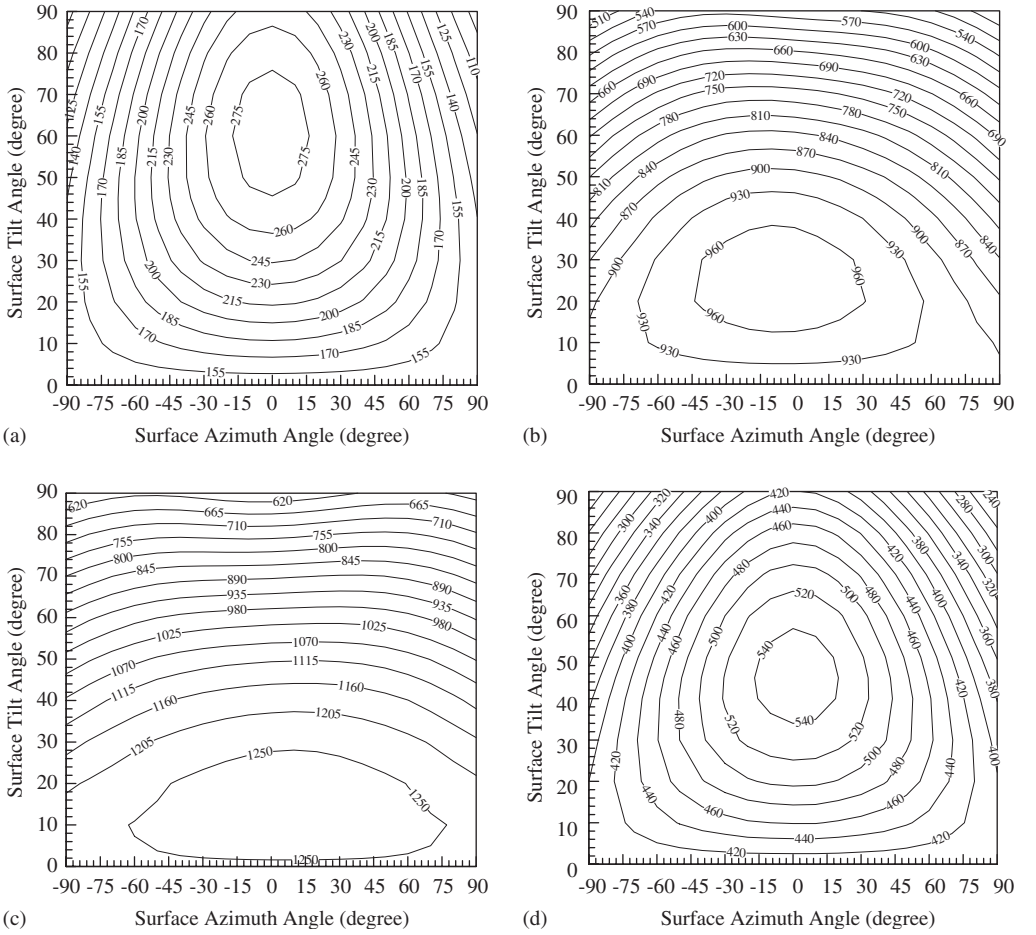

Fig. 8. Seasonal PV output for any surface normalised with respect to PV rated capacity (MJ kW_p^{-1}): (a) winter, (b) spring, (c) summer and (d) autumn.

duration are smaller than summer (see Fig. 1). The surface with larger tilt angle is therefore more perpendicular to the horizon than the one with smaller installation angle and thus receives more insolation during winter. In summer, the maximum PV output is for a surface with tilt and azimuth angles of 10° and 0°, respectively. When the optimum orientation and inclination for winter is considered, the reduction in the annual PV output is 16% compared with the optimum orientation and inclination on annual basis. Similarly for summer, the reduction is 2.3%. In spring, the PV output is maximised for a surface with tilt angle of 30° oriented 10° east of south. The maximum PV output is for the orientation slightly east of due south which is due to an asymmetric distribution of insolation before and after the midday during this season. However, the PV output varies only by 1.5% from the maximum PV output in this season, when the PV surface orientation lies within 30° east or west from due south. For south-facing horizontal and vertical surfaces, PV outputs are 7.3% and 53% lower, respectively, than the maximum PV output in spring. In autumn, the maximum PV output is found for a 50°-tilted surface

facing south and for south-facing horizontal and vertical surfaces, PV outputs decline approximately by 27%.

6. Effect of surface inclination and orientation on PV efficiency

PV efficiency for any surface azimuth and tilt angles, $\eta_{\mathrm{PV},\gamma,\beta}$ is calculated from

$$\eta_{\mathrm{PV},\gamma,\beta} = \frac{E_{\mathrm{DC},\gamma,\beta}}{I_{\gamma,\beta}A} \times 100\%, \tag{7}$$

where A is the area of the PV array.

The annual PV efficiency calculated from annual total insolation and annual PV output for various surface tilt and azimuth angles is shown in Fig. 9. The maximum annual PV efficiency is 10.4% for a south-facing surface with a tilt angle of 20° and the minimum is 8.25% for a vertical surface with orientation of 90° west or east from due south. For lower tilt angles, the variation of annual PV efficiency with respect to surface azimuth angles is insignificant. For horizontal and vertical surfaces, the annual PV efficiencies are approximately 1.2% and 15.5% lower, respectively, than the annual maximum.

Fig. 10 illustrates the monthly variation of PV efficiency for a south-facing surface with respect to various surface inclinations. For a horizontal surface, the monthly PV efficiency varies from 7.87% to 10.74% over a year and for vertical surface from 8.11% to 9.88%. The maximum monthly PV efficiency is 10.75% in June for a surface with a tilt angle of 10° and the minimum is 7.87% in December for a horizontal surface. The maximum annual

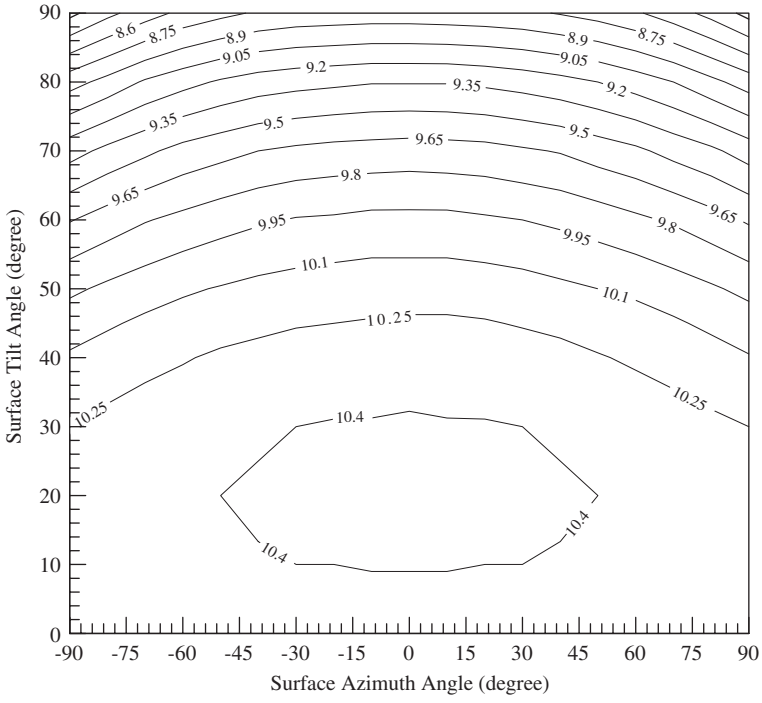

Fig. 9. Variation of annual PV efficiency as functions of surface azimuth and tilt angles.

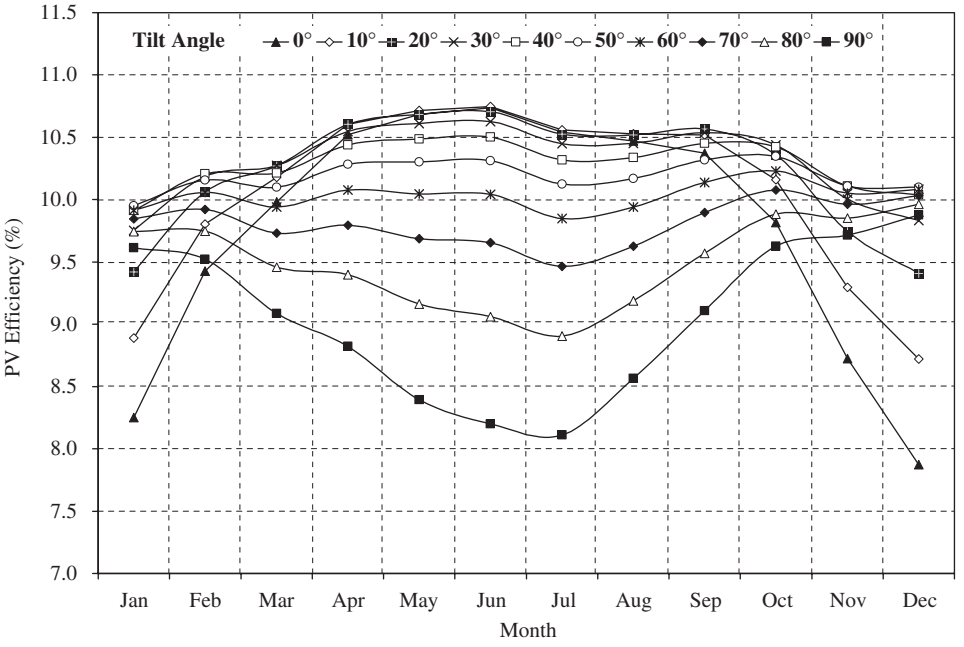

Fig. 10. Variation of monthly PV efficiency as a function of surface tilt angle for a south-facing surface.

average monthly PV efficiency is 9.97% for a surface with a tilt angle of 10° and the minimum is 9.1% for a vertical surface, 8.8% lower than the maximum average value. The maximum variation of monthly PV efficiency over a year is 26.7% for a horizontal surface and the minimum is 3.6% for a 60°-tilted surface, signifying that the effect of tilt angle on the performance of a PV array is significant for lower surface inclinations.

7. Effect of surface inclination and orientation on inverter efficiency

The inverter efficiency for any surface azimuth and tilt angles, $\eta_{\text{inv},\gamma,\beta}$ is calculated from

$$\eta_{\text{inv},\gamma,\beta} = \frac{E_{\text{AC},\gamma,\beta}}{E_{\text{DC},\gamma,\beta}} \times 100\%, \tag{8}$$

where $E_{\text{AC},\gamma,\beta}$ is the inverter output for any surface azimuth. The annual inverter efficiency for any surface orientation and inclination is calculated from annual total AC and DC outputs for that surface and monthly inverter efficiency from monthly total AC and DC outputs.

Fig. 11 shows annual inverter efficiency as functions of surface azimuth and tilt angles. The maximum annual inverter efficiency is 87.3% for a surface with tilt and azimuth angles of 20° and 0°, respectively and the minimum is 81.6% for a vertical surface with orientation 90° east from south. For south-facing horizontal and vertical surfaces, the annual inverter efficiencies decline by 0.36% and 2.98%, respectively, from the annual maximum value. It is found that if the annual inverter efficiency for any surface is normalised with respect to the maximum annual value (i.e., 87.3%), the normalised factor

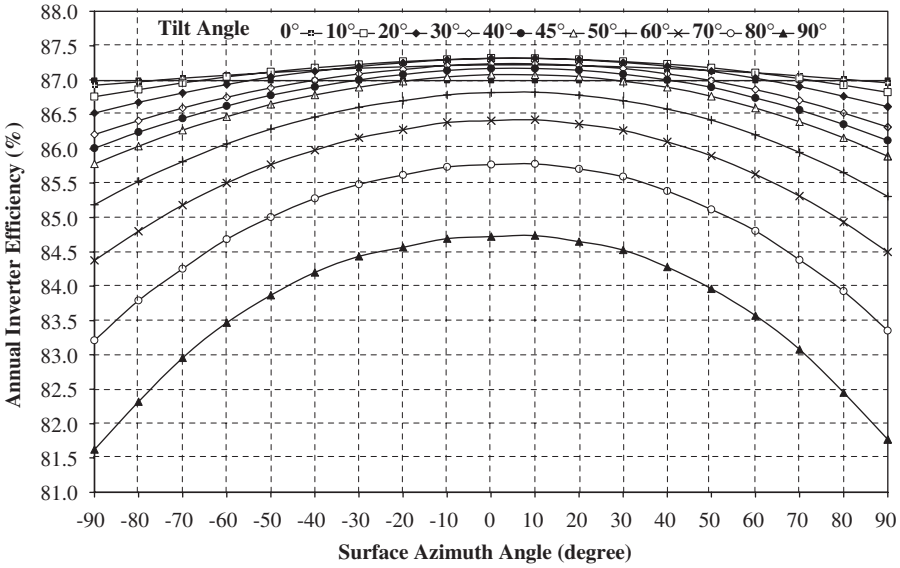

Fig. 11. Variation of annual inverter efficiency as functions of surface azimuth and tilt angles.

lies within 0.935–1.00. Due to the variation of orientation from south to 90° east or west, the normalised factor varies from 0.935 to 0.970 for vertical surface, 0.987–0.999 for 40° tilted surface and 0.995–0.999 for 10° tilted surface signifying that the annual inverter performance is less affected by the variation of surface azimuth angle for surfaces with lower tilt angles from the horizontal.

Fig. 12 illustrates the monthly variation of inverter efficiency for a south-facing surface with respect to various surface tilt angles. The maximum monthly inverter efficiency is found to be 88.7% for a horizontal surface in June; 25% higher than the minimum value obtained for the same surface in December. The average monthly maximum and minimum inverter efficiencies are 86.2% and 82.6% for surface with tilt angles of 50° and 0°, respectively. For horizontal surface, the inverter efficiency during winter months is significantly lower compared to the other surface inclinations. This is because during winter months, the PV generation is very low for lower surface inclinations and thus inverter operates mostly under its rated capacity causing reduction in inverter efficiency. For a vertical surface, the monthly inverter efficiency varies only 3.1% over a year indicating that the inverter performance is consistent over the year.

8. Effect of surface inclination and orientation on overall system efficiency

The overall system efficiency for any surface azimuth and tilt angles, $\eta_{s,\gamma,\beta}$, is calculated as follows:

$$\eta_{s,\gamma,\beta} = \frac{E_{AC,\gamma,\beta}}{I_{\gamma,\beta} A} \times 100\%. \tag{9}$$

The annual overall system efficiency as functions of surface azimuth and tilt angles is shown in Fig. 13. The maximum annual overall system efficiency is 9.13% for a surface

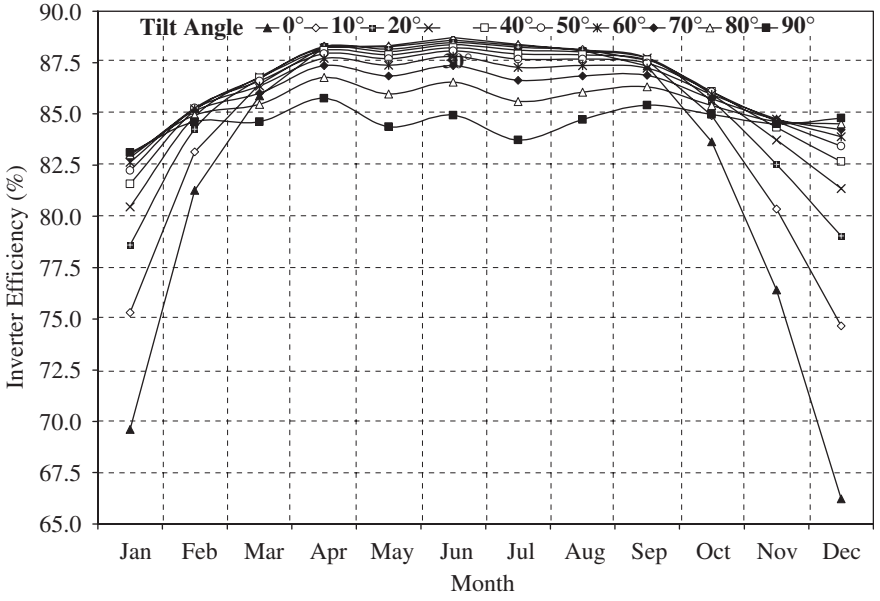

Fig. 12. Variation of monthly inverter efficiency as a function of surface tilt angle for a south-facing surface.

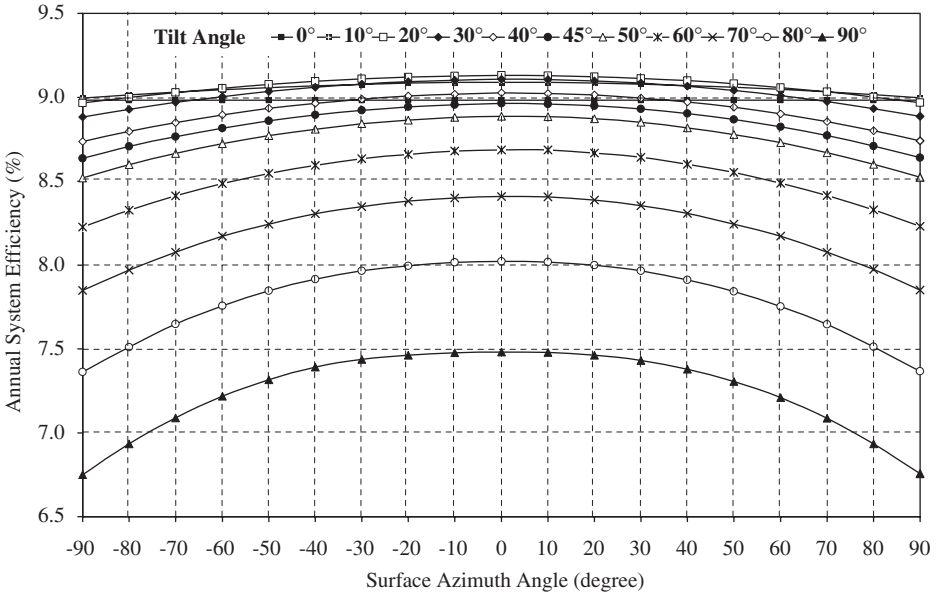

Fig. 13. Variation of annual system efficiency as functions of surface azimuth and tilt angles.

with tilt and azimuth angles of 20° and 0°, respectively, and minimum is 6.75% for a vertical surface with orientation of 90° east or west form south. For south-facing horizontal and vertical surfaces, the annual overall system efficiencies are reduced by 1.6%

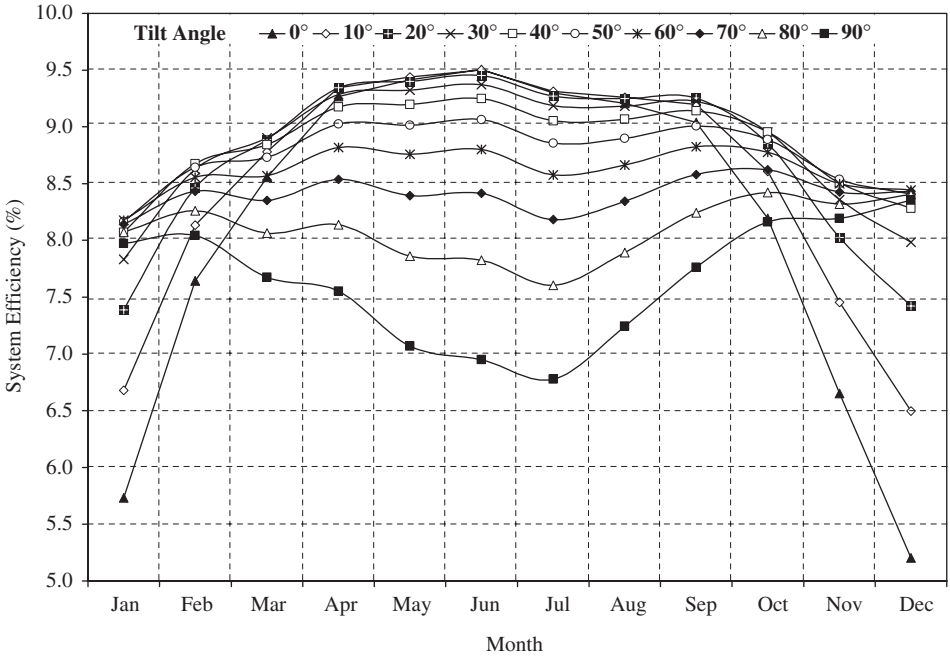

Fig. 14. Variation of monthly system efficiency as a function of surface tilt angle for a south-facing surface.

and 18.1%, respectively. Due to the variation of PV surface orientation from south to 90° east or west, the annual overall system efficiency varies approximately by 1.0% for a 10°-tilted surface and 9.8% for a vertical surface.

The monthly variation of overall system efficiency for a south-facing surface with respect to tilt angles depicted in Fig. 14 shows that the maximum monthly overall system efficiency is 9.5% in June for a surface inclined at 10° and the minimum is 5.2% in December for a horizontal surface, approximately 45% lower than the maximum value. The maximum and minimum average monthly overall system efficiencies are 8.6% and 6.8% for surface inclination of 30° and 90°, respectively.

9. Effect of surface inclination and orientation on PR

PR is defined as the ratio of final yield, Y_f, to reference yield, Y_r, and is given as follows:

$$\mathrm{PR} = \frac{Y_f}{Y_r} \times 100\%. \tag{10}$$

PR allows comparison of PV systems independent of location, tilt angle and orientation and their nominal power [20]. The annual system PR calculated from annual final and reference yields for various surface orientations and inclinations is shown in Fig. 15. The maximum annual system PR is 72.3% for a surface with tilt and azimuth angles of 20° and 0°, respectively. For horizontal and vertical south-facing surfaces, the system PR are 71.1% and 59.2%, respectively, which are 1.65% and 18.1% lower than maximum value. The lowest system PR is found to be 53.5% for a vertical surface with an orientation of 90°

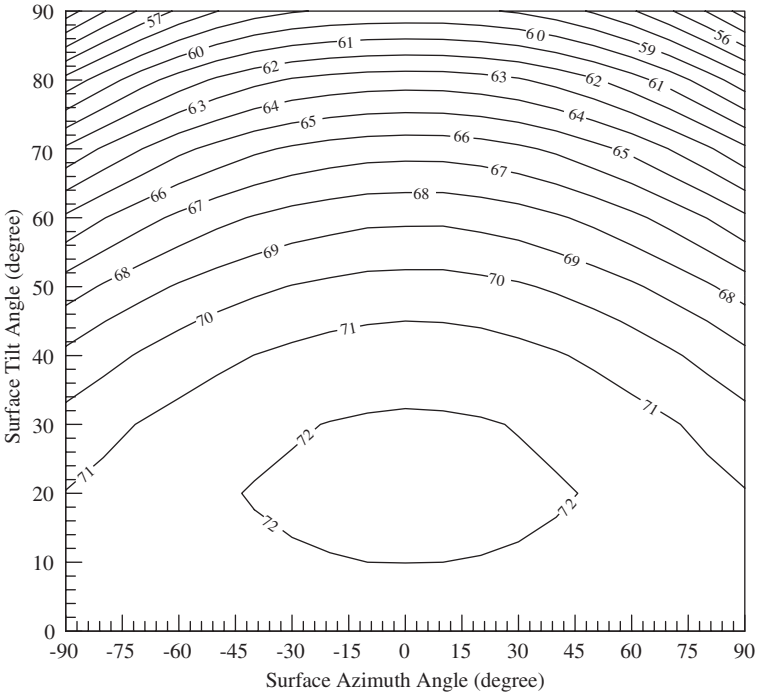

Fig. 15. Distribution of annual system performance ratio as functions of surface azimuth and tilt angles.

east or west from due south. The system PR is affected by these surface orientations and inclinations due to the PV system operation under low insolation conditions, which affects the performance of both the PV and the inverter, and the overall system PR thus declines.

The monthly variation of system PR as a function of surface tilt angle for a south-facing surface is shown in Fig. 16. For a horizontal surface, the lowest system PR is in December with 41.2% and increases to 75.3% in June resulting in a variation of 45.2% over a year; on the contrary, for a vertical surface, the minimum system PR is 53.7% in July and the maximum 66.2% is in December, resulting in an annual variation of 18.8%. For 50° and 60° tilted surfaces, the monthly variation of system PR over a year are approximately 9.8% and 7.3%, respectively, whereas for 20° and 40° tilted surfaces, the corresponding variations are 21.8% and 12.7%, respectively. For lower surface tilt angels, the system PR increases in summer but decreases significantly in winter. The results show that during summer, the system PR varies slightly for surface tilt angles between 10° and 30°.

10. Effect of surface inclination and orientation on PV savings

Fig. 17 illustrates annual PV savings for two utility tariff rates as functions of surface azimuth and tilt angles. For utility tariff 1, the maximum annual PV savings is 657 £ kW_p^{-1} for a surface with tilt and azimuth angles of 30° and 10°, respectively, whereas for tariff 2, the maximum is 1052 £ kW_p^{-1} for 30° and 0°. The results show that for tariff 1, the annual PV savings is always higher for any tilted surface facing the same angle towards west than east from south due to the time-dependent seasonal utility rate. Table 2 shows that the

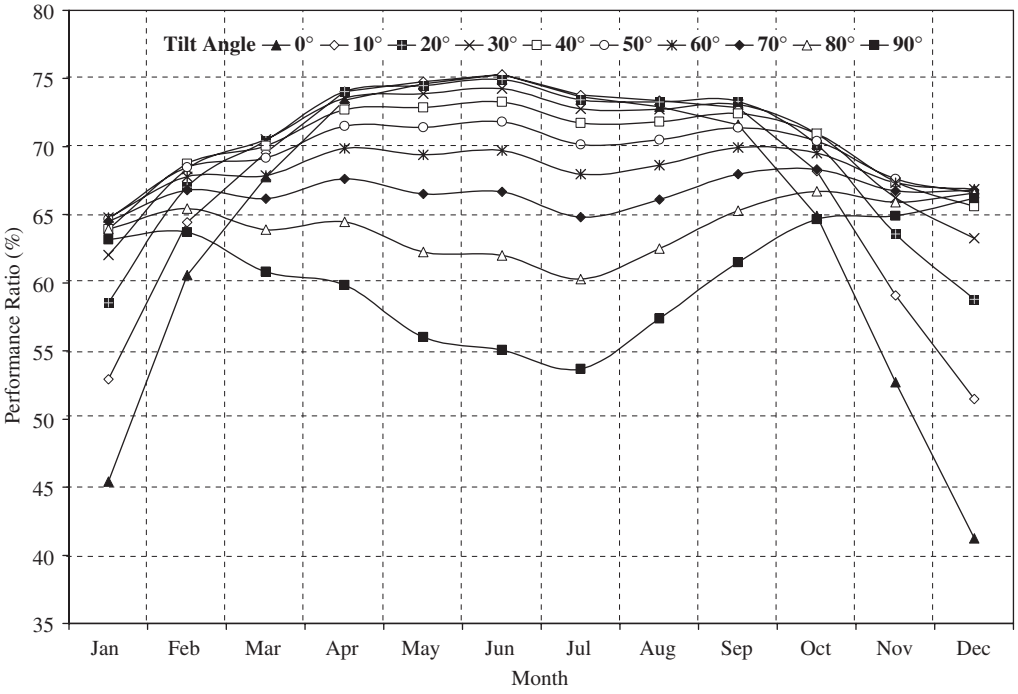

Fig. 16. Variation of monthly system performance ratio as a function of surface tilt angle for a south-facing surface.

utility rate is significantly higher in winter than in summer during the period from 4 to 7 pm, therefore, the annual PV savings for a west-facing surface is higher than for an east-facing surface even when PV generation is the same for surfaces with same orientation east or west from south. For example, the annual PV savings for vertical surface with orientation of 90° east from south is 7.9% lower than for 90° west, and for 10° tilted surface it is 1.0% lower. On the other hand, for tariff 2, the annual PV savings is the same for the same orientation towards east and west from south due to constant tariff rate over the year. For a horizontal south-facing surface, the annual PV savings is 12.9% and 9.9% lower than the maximum annual PV savings for tariffs 1 and 2, respectively, and for a vertical surface it is lower by 38.0% and 39.6%, respectively.

11. Conclusions

The performance of a grid-connected PV system for various PV surface orientations and inclinations has been investigated under maritime climates using a validated TRNSYS model. The maximum annual insolation and PV output were found to be for a south-facing surface with an inclination of 30°. The monthly optimum collection angle for a south-facing surface maximising incident insolation varied from 10° in June to 70° in December and seasonally from 20° in summer to 60° in winter. The annual incident insolation on horizontal and vertical surfaces with orientations of 90° east or west from due south were 9.0% and 42.5% lower, respectively, than the maximum annual insolation,

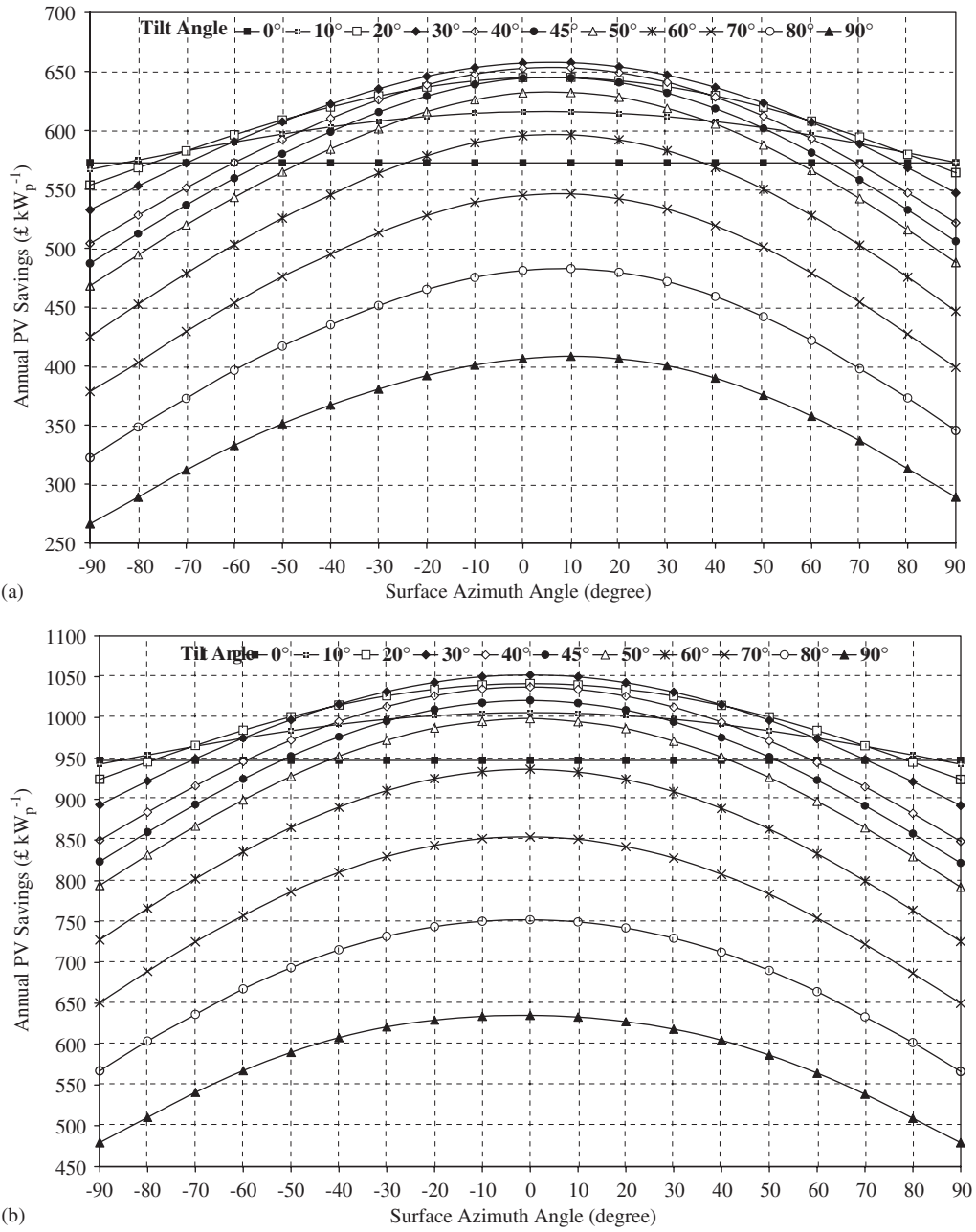

Fig. 17. Variation of annual PV savings as functions surface azimuth and tilt angles: (a) Tariff 1 and (b) Tariff 2.

and annual PV outputs were 9.9% and 54.4% lower, respectively than the annual maximum total PV output. It was found that PV and inverter efficiencies, and hence system efficiency and PR varied with respect to surface orientation and inclination.

The maximum annual PV and inverter efficiencies were found to be for a south-facing surface inclined at 20° and the minimum was for a vertical surface facing 90° east or west from south. Over a year, the maximum monthly variation of PV and inverter efficiencies and therefore system PR are found for a horizontal surface and the minimum is for a surface with inclination in the range 50–60°. Tariff rates affect the optimum surface orientation and inclination of a grid-connected PV system; due to the time dependent tariff rate, the annual PV savings is always higher for a surface with the same orientation towards west than east from due south but for a constant tariff rate, the annual PV savings is symmetric towards east or west orientation from due south. For time-dependent tariff rates, the maximum annual PV savings was found for a surface with inclination and orientation angle of 30° and 10° west from south, respectively, and for a constant tariff rates, the maximum was for the same inclination but orientation due south.

Acknowledgement

This work is supported by the UK Department of Trade and Industry.

References

[1] Tsalides P, Thanailakis A. Direct computation of the array optimum tilt angle in constant-tilt photovoltaic systems. Sol Cells 1985;14:83–94.
[2] Kern J, Harris I. On the optimum tilt of a solar collector. Sol Energy 1975;17:97–102.
[3] Bari S. Optimum slope angle and orientation of solar collectors for different periods of possible utilization. Energy Convers Manage 2000;41:855–60.
[4] Duffie JA, Beckman WA. Solar engineering of thermal processes, 2nd ed. Wiley; 1991.
[5] Helmke C, Jantsch M, Ossenbrink HA. The large amorphous silicon PV façade in ISPRA experience and results after one year of operation. In: The 13th European photovoltaic solar energy conference, Nice, France, 1995. p. 695–98.
[6] Nakamura H, Yamada T, Sugiura T, Sakuta K, Kurokawa K. Data analysis on solar irradiance and performance characteristics of solar modules with a test facility of various tilted angles and directions. Sol Energy Mater Sol Cells 2001;67:591–600.
[7] Soleimani EA, Farhangi S, Zabihi MS. The effect of tilt angle, air pollution on performance of photovoltaic systems in Tehran. Renew Energy 2001;24:459–68.
[8] Oladiran MT. Mean global radiation captured by inclined collectors at various surface azimuth angles in Nigeria. Appl Energy 1995;52:317–30.
[9] Akhmad K, Belley F, Kitamura A, Yamamoto F, Akita S. Effect of installation conditions on the output characteristics of photovoltaic modules. In: IEEE photovoltaic specialists conference, Hawaii, 1994. p. 730–3.
[10] Hiraoka S, Fujii T, Takakura H, Hamakawa Y. Tilt angle dependence of output power in an 80 kWp hybrid PV system installed at Shiga in Japan. Sol Energy Mater Sol Cells 2003;75:781–6.
[11] Balouktsis A, Tsanakas D, Vachtsevanos G. On the optimum tilt angle of a photovoltaic array. Int J Sol Energy 1987;5:153–69.
[12] Kacira M, Simsek M, Babur Y, Demirkol S. Determining optimum tilt angles and orientations of photovoltaic panels in Sanliurfa, Turkey. Renew Energy 2004;29:1265–75.
[13] Hussein HMS, Ahmad GE, El-Ghetany HH. Performance evaluation of photovoltaic modules at different tilt angles and orientations. Energy Convers Manage 2004;45:2441–52.
[14] Mondol JD. Long-term performance analysis, simulation, optimisation and economic analysis of a building-integrated photovoltaic system. PhD thesis, Faculty of Engineering, University of Ulster, UK, 2004.
[15] Klein, et al. TRNSYS 15, A transient simulation program. Madison, WI: Solar Energy Laboratory; 2000.
[16] Liu BYH, Jordan RC. The interrelationship and characteristic distribution of direct, diffuse and total solar radiation. Sol Energy 1960;4:1–19.
[17] Mondol JD, Yohanis YG, Smyth M, Norton B. Long-term validated simulation of a building integrated photovoltaic system. Sol Energy 2005;78:163–76.

[18] Anon. Home energy and business energy prices—2004, Northern Ireland Electricity, 2004.
[19] Mondol JD, Yohanis YG, Smyth M, Norton B. Performance analysis of a grid-connected building integrated photovoltaic system. In: ISES solar world congress, Göteborg, Sweden, 14–19 June 2003 (CD-version).
[20] Decker B, Jahn U. Performance of 170 grid connected PV plants in Northern Germany—analysis of yields and optimization potentials. Sol Energy 1997;59:127–33.